**Proceedings of the Institute of Acoustics**

# NETWORK REPRESENTATION OF THE MIDDLE AND INNER EAR IN A COMPOSITE MODEL OF THE AUDITORY PERIPHERY

C. Giguère and P.C. Woodland

Cambridge University Engineering Department, Trumpington Street, Cambridge CB2 1PZ

## 1. INTRODUCTION

A composite model of the auditory periphery assembled from submodels of the relevant anatomical structures of the outer, middle and inner ear has recently been described [2, 3]. The submodels can be equivalently represented as lumped-element electrical networks or as wave digital filters. The equivalence follows from the property of wave digital filters to preserve the precise topology of the analog systems to be simulated (see [1] for a review of this class of digital filters). While the electrical network representation is useful at the design stage of model development, the wave digital filter representation provides computationally-efficient time-domain numerical solutions.

In the first version of the model [2, 3], the outer ear and middle ear modules are bidirectionally interconnected, but the inner ear modules are implemented separately in series. A basilar membrane (BM) module incorporates the effect of outer hair cells (OHCs) as mechanical force generators acting on the cochlear partition. The net pressure developed by the OHCs is approximated by a voltage source in each shunt branch of an otherwise classical transmission line network of cochlear hydrodynamics/basilar membrane motion. By injecting energy in phase with basilar membrane velocity at low levels, the OHC circuit leads to auditory filters with level-dependent frequency selectivity and sensitivity. A functional feedback unit regulates the firing activity at the output of an inner hair cell (IHC) transduction module via a simplified modelling of the dynamics of the descending pathways.

This article describes recent improvements made to the peripheral model. The BM-OHC module is now bidirectionally interconnected to the middle ear module. The ascending path of the model is thus fully coupled, except for IHC transduction. It opens new applications of the model in hearing research while remaining computationally attractive for speech research. The parameter values of the BM-OHC module have been reviewed to achieve a more realistic set of level-dependent basilar membrane tuning curves reproducing the observed basal shift of characteristic place at high levels for fixed frequencies. The effects of spatial discretization of the basilar membrane are discussed.

## 2. MIDDLE EAR NETWORK

Electrical networks provide a very compact way of representing the equations of motion of complex mechanoacoustical systems such as the middle ear. In the voltage-pressure electroacoustic analogy, inductors, resistors and capacitors of a given electrical network are analogous to the acoustic mass, resistance and compliance components of the modelled system. Electrical voltage and current variables correspond to acoustic pressure and volume velocity acting on or flowing through a particular cross-section of the acoustic system.

# NETWORK REPRESENTATION OF MIDDLE AND INNER EAR

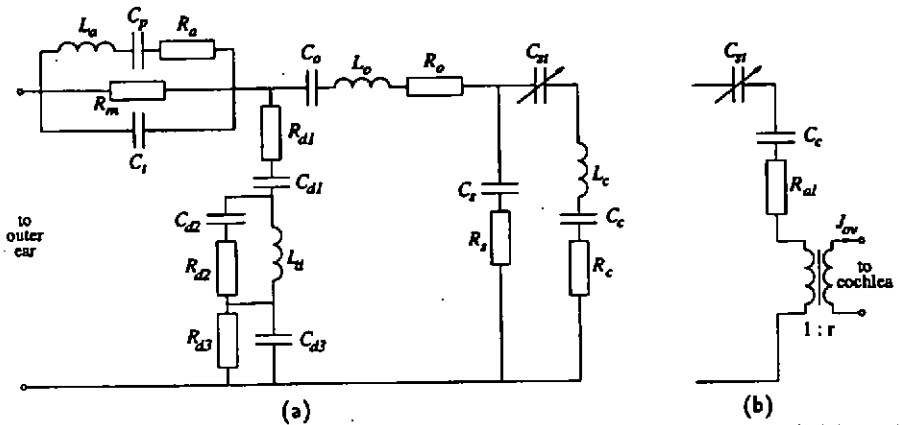


Figure 1. Network representation of the middle ear: (a) model of Lutman and Martin [6], (b) modified terminal branch with explicit connection to cochlea.

The electroacoustic network model of the middle ear of Lutman and Martin [6] is shown in Fig. 1*a*. It is an adaptation of the network of Zwislocki [10] that includes the terminal effect of the stapedial muscle contractions as an explicit electrical element. The set of elements $\{L_a, C_p, R_a, R_m, C_t\}$ models the impedance of the middle ear cavities behind the eardrum. The central part of the eardrum, and the malleus and incus ossicles of the middle ear appear to be rigidly attached mechanically. Their contributions are combined as one set of elements $\{C_o, L_o, R_o\}$. The edges of the eardrum are not coupled directly to the malleus and this is modelled by a shunt branch with elements $\{R_{d1}, C_{d1}, C_{d2}, R_{d2}, L_d, R_{d3}, C_{d3}\}$. Likewise, some energy is lost at the incudo-stapedial joint and this is represented by the shunt branch with elements $\{C_s, R_s\}$. The contributions of the stapes, oval and round windows, and cochlear input impedance are all lumped together in three elements $\{L_c, C_c, R_c\}$. Finally, the time-variant capacitor $C_{st}(t)$ models the variable compliance of the stapes suspension in response to stapedial muscle contractions.

In [2, 3], the network of Lutman and Martin was selected as the middle ear module of the peripheral model. In the present study, to obtain a fully-coupled peripheral ear, the terminal branch of their network is modified as shown in Fig. 1*b* to allow the cochlea to be explicitly represented. The current variable $J_{ov}(t)$ is the volume velocity of the stapes footplate in the oval window of the cochlea. The BM-OHC network module (Fig. 2) is connected to the middle ear through an ideal transformer of ratio r = 30 representing the effective mechanoacoustical impedance transformation between the eardrum and the oval window. Element $R_{al} = 100\Omega$ represents the resistance of the annular ligaments at the oval window. Based on the experimental data of Lynch *et al.* [7], the value for $R_{al}$ was chosen as about 1/6 of the real part of the cochlear input impedance at mid-frequencies when referred to the impedance at the eardrum, i.e. calculated from the left side of the transformer. Capacitor $C_c = 0.6\mu$F corresponds to the compliance at the oval and round windows. As in Lutman and Martin [6], the time-variant capacitor $C_{st}(t)$ represents the effect of stapedial muscle contractions. The terminal branch should also include a series inductor to account for the mass of the stapes. Its contribution, however, would be very small compared to the imaginary part of the cochlear input impedance and was neglected.

## 3. BASILAR MEMBRANE AND OUTER HAIR CELL NETWORK

The BM-OHC transmission line network is shown in Fig. 2. The membrane is discretized into N segments of equal length $\Delta x$. To establish a correspondence between segment place $x_n$ (cm) and characteristic frequency $f_n$ (Hz) and to eliminate the potential problem of apical reflections [9], the cochlear mapping function of Greenwood [4] is used:

$$x_n = 3.5 - \frac{1}{0.6}\log(\frac{f_n}{165.4} + 1). \tag{1}$$

The membrane is not modelled over its entire length of 3.5 cm. Rather, the end points $x_1 = 0.23$ cm and $x_N = 3.42$ cm of the line span the maximum $f_1 = 15000$ Hz and minimum $f_N = 20$ Hz desired auditory filter characteristic frequencies. The network elements are derived from electroacoustic analogies and from the assumption that the natural frequency of the shunt second-order resonant circuit in each segment is equal to the characteristic frequency of the BM at that place:

$$L_{sn} = \frac{2\rho\Delta x}{A(x_n)} \qquad L_n = \frac{M}{b(x_n)\,\Delta x} \qquad C_n = \frac{1}{4\pi^2 f_n^2 L_n} \qquad R_n = Q^{-1}\sqrt{\frac{L_n}{C_n}} \tag{2}$$

where $\rho = 1.0$ g/cm$^3$ is the fluid density, $A(x) = 0.03\ e^{-0.6x}$ cm$^2$ is the cross-sectional area of the cochlear ducts, $M = 0.015$ g/cm$^2$ is the transversal mass per area of BM, $b(x) = 0.015\ e^{0.3x}$ cm is the BM width, and $Q = 2$ is the quality factor of the shunt resonant circuit. The line is terminated by an inductor $L_T$ representing the acoustic mass of cochlear fluid from the end of the last segment ($x = x_N + \Delta x$) to the helicotrema ($x = 3.5$ cm), the latter being modelled as a short-circuit.

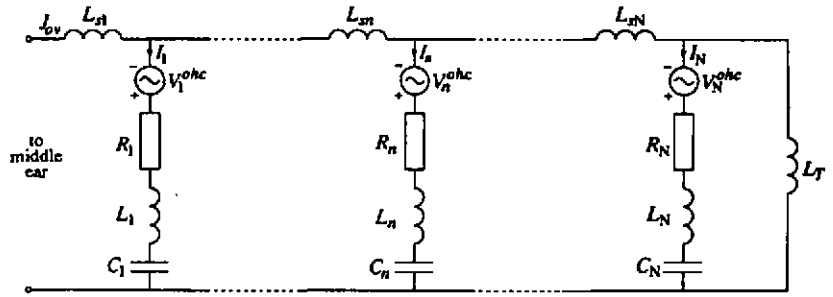


Figure 2. Network representation of the BM and OHCs.

The pressure developed by the OHCs and acting on the cochlear partition is represented in each shunt branch by a level-dependent voltage source saturating at high levels as follows:

$$V_n^{ohc}(t) \;=\; G\,R_n\left(\frac{d_{1/2}}{d_{1/2} + |d_n(t)|}\right) I_n(t) \tag{3}$$

where $G = 0.99$ is a gain factor, $d_n(t)$ is the BM displacement and $d_{1/2}$ is the half-saturating point of the nonlinearity. The proportionality of $V_n^{ohc}(t)$ with BM volume velocity $I_n(t)$ implies that the effect of the OHCs is undamping. The network is scaled by assuming that an incident sinusoidal wavefront of 50 dB (SPL) at 1000 Hz is associated with a BM displacement (rms) of $d_{1/2}$ at the place of resonance along the BM. The output is the BM particle velocity $i_n(t) = I_n(t)/(b(x_n)\Delta x)$.

## 4. RESPONSE CURVES

### 4.1 Input Impedance

The acoustic input impedance of the BM-OHC network is shown in Fig. 3 for different parameter values. Because source $V_n^{ohc}(t)$ makes the network nonlinear with level, the OHCs are disconnected (i.e. $G = 0$) for these calculations. Note from Sec. 3 that the main contribution of $V_n^{ohc}(t)$ is to reduce the real part the BM point impedance at low levels. The effect of the OHCs on the input load of the BM-OHC network can be approximated at different levels by increasing the quality factor $Q$ in Eqn. 2 from its standard value of 2. The input impedance is then calculated in the frequency-domain by use of Laplace transform applied to the resulting linear network.

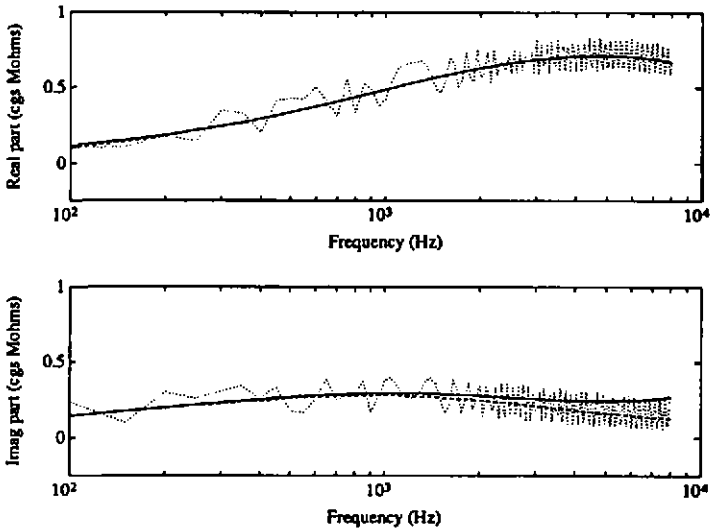


Figure 3. Input impedance of BM-OHC network for $\{Q = 2, N = 128, G = 0\}$ (solid line), $\{Q = 30, N = 128, G = 0\}$ (dotted line), and $\{Q = 30, N = 320, G = 0\}$ (dashed line). Divide by $r^2 = 900$ to obtain input impedance referred to the left side of the middle ear transformer.

The set of curves $\{Q = 2, N = 128, G = 0\}$ approximates the input load of the BM-OHC network at high levels (>90 dB). The real part of the input impedance increases monotonically until it reaches a peak of 0.71 MΩ at 4900 Hz. The imaginary part is almost flat from 100 to 8000 Hz with a very broad peak of 0.30 MΩ around 1100 Hz. The impedance magnitude (not shown) is 0.57 MΩ at 1000 Hz and peaks at 4900 Hz where it reaches 0.75 MΩ. The impedance phase (not shown) is about 50° at 100 Hz and decreases gradually to the range 16–20° above 3000 Hz. These values are in general agreement with the model calculations and human data reported in Puria and Allen [9]. We also refer to their paper for a detailed parametric study of cochlear input impedance.

The set of curves $\{Q = 30, N = 128, G = 0\}$ in Fig. 3 approximates the input load of the BM-OHC network at low levels ($\simeq$ 10–20 dB). The real and imaginary parts of the input impedance exhibit oscillations over the entire frequency range plotted. The oscillations are eliminated if the number of

BM segments is increased from 128 to 320 as shown by the set of curves $\{Q = 30, \mathrm{N} = 320, G = 0\}$. On Greenwood cochlear map, this corresponds to increasing the density of segments from 4 to 10 per critical band. Thus, the input impedance oscillations are not due to apical reflections; we are using a cochlear map of the recommended type in [9] and the apical boundary $f_N$ of the network extends well below 100 Hz. Rather, there is a partial reflection of the forward travelling wave at each segment boundary leading to the presence of standing waves along the cochlea. The amount of reflection at a given place along the network depends on the steepness of BM point impedance change across neighbouring segments. In particular, if $Q$ is high (i.e. low level) and the BM discretization is coarse, there is an abrupt phase flip of 180° at the characteristic frequency.

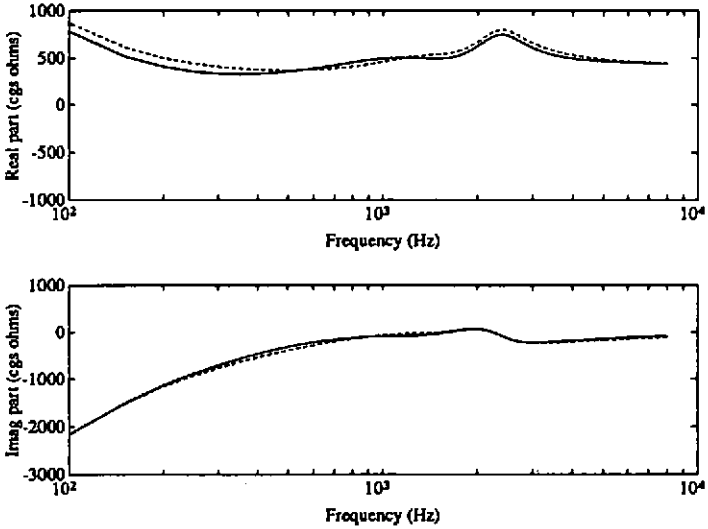


Figure 4. Input impedance of the middle ear network $\{Q = 2, \mathrm{N} = 128, G = 0, C_{at} = \infty\}$ (solid line) compared to that of the original network of Lutman and Martin [6] (dashed line).

The acoustic input impedance of the middle ear network with connected BM-OHC network is shown in Fig. 4 for the set of parameter values $\{Q = 2, \mathrm{N} = 128, G = 0\}$. There is a very good agreement with the input impedance of the original middle ear model of Lutman and Martin for both the real and imaginary parts. Increasing the quality factor $Q$ from 2 to 30 (not shown) results in small oscillations of the input impedance. The effect is much less pronounced than in Fig. 3 and is limited to the frequency range 200–1500 Hz where the cochlea most influences middle ear input impedance. Again, increasing the number of BM segments from 128 to 320 eliminates oscillations.

### 4.2 Transmission Characteristics

The response of the peripheral model from the free field to the basilar membrane is illustrated in this section. For this purpose, the middle ear network is connected at its input to a network model of the outer ear. The resulting model is implemented in the time-domain by translating the coupled outer ear, middle ear and BM-OHC networks into wave digital filters. The rate of operation of the

filters is 48000 Hz. For realizability, the computation of $V_n^{ohc}(t)$ is delayed by one sampling interval. The effect of stapedial muscle contractions is not considered here, i.e. $C_{st}(t) = \infty$. We refer to [2, 3] for details of the outer ear network, the operation of the stapedial muscle and acoustic reflex, and the wave digital filter representation of a previous version the model.

Fig. 5*a* presents the response of the model as a function of place $x$ along the basilar membrane for a pure tone of 1000 Hz at different free-field input levels. The amplitude of the travelling wave increases slowly from the basal end of the cochlea ($x = 0$) to the place of resonance ($x \simeq 2.0$ cm) and decreases very rapidly afterwards. At low input levels, the BM is sharply tuned showing great frequency selectivity. The standing waves referred to in Sec. 4.1 are clearly seen on the basal skirt of the low-level curves when N=128. They are greatly reduced if the number of BM segments is increased to 320. At high input levels, the OHCs are saturated. The BM becomes much more broadly tuned and the place of resonance moves basally by 0.225 cm, a shift equivalent to about 1/2-octave on the cochlear map. The same amount of shift is reported in [5] for the real cochlea.

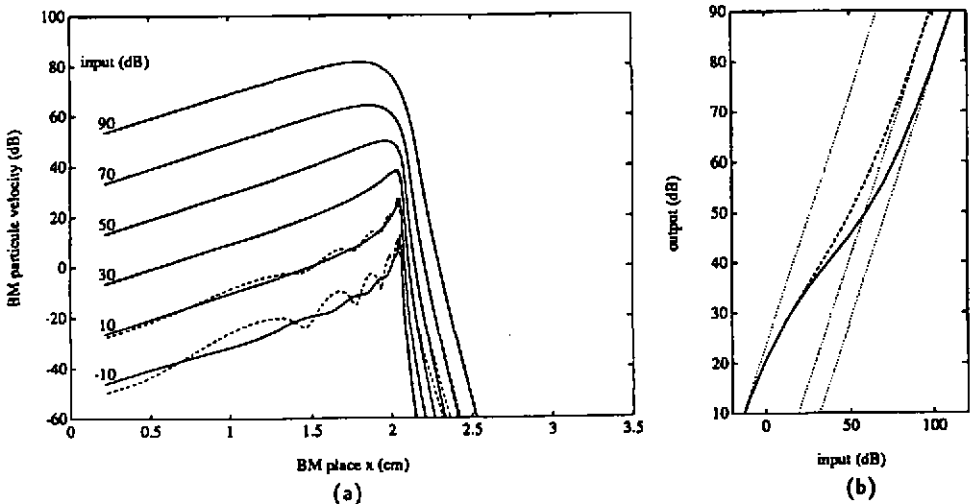


Figure 5. BM place response to a pure tone of 1000 Hz at different input levels: (a) envelope curves for N = 320 (solid line) and N = 128 (dashed line), (b) input–output response at place $x = 2.06$ cm (solid line) and along the locus of maximum vibration (dashed line).

Fig. 5*b* illustrates the level-dependent sensitivity of the BM near resonance by plotting the free-field input level against the BM velocity output (in dB) at a fixed place ($x = 2.06$ cm, CF $\simeq$ 1000 Hz) and along the locus of maximum vibration irrespective of place. At low (< 10 dB) and high (> 90 dB) input levels, the basilar membrane behaves linearly, i.e. both input-output curves converge towards the dotted asymptotes with slopes of 1. At mid-frequencies, the BM is compressive. The amount of level compression, the horizontal distance between asymptotes, is 43 dB at fixed place $x = 2.06$ cm and 31 dB along the locus of maximum vibration. The former value is larger because of the basal shift of characteristic place. In contrast, corresponding compression values of 55 dB and 40 dB can be inferred for the real cochlea from the data reported in [5].

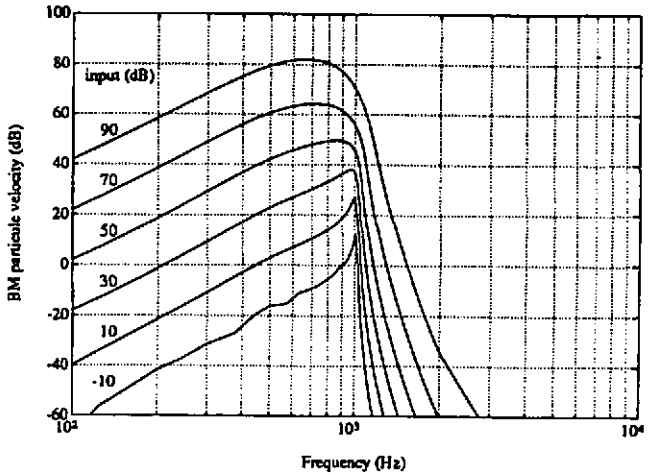


Figure 6. BM frequency response at place $x = 2.06$ cm for different input levels ($N = 320$).

Fig. 6 presents the response of the model in the more conventional way of plotting the BM particle velocity at a given place ($x = 2.06$ cm, CF $\simeq$ 1000 Hz) for a range of frequencies and input levels. Essentially the same conclusions as those drawn for Fig. 5*a* apply. The characteristic frequency decreases from 1000 Hz at low levels to 667 Hz at high levels, a shift of about 1/2-octave. The amount of compression is 43 dB at 1000 Hz and is 31 dB along the locus of maximum vibration. Note that the input level is referred to the free field, and thus, the transmission characteristics of the outer and middle ear (Fig. 7) are included in these curves.

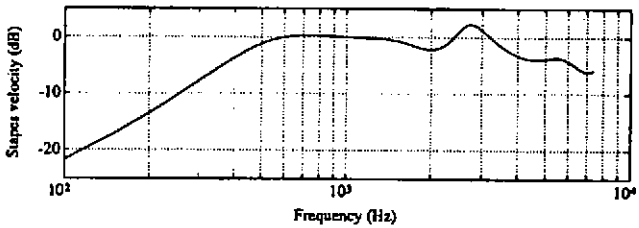


Figure 7. Transmission characteristics of the outer and middle ear networks $\{G = 0, C_{et} = \infty\}$.

## 5. CONCLUSIONS

This paper described an improved version of our auditory model with coupled outer ear, middle ear and cochlear mechanics. It allows the computation of both forward and backward waves through the peripheral ear. This opens new applications of the model such as studies of otoacoustic emissions and cochlear reflections. The spatial discretization effects of the basilar membrane — local reflections, standing waves, input impedance oscillations — must be carefully taken into account for

such applications. Note that the basilar membrane is not a fully homogeneous medium and there are only a finite number of OHC attachment points to the tectoral membrane. Minute reflections are therefore to be expected in the real cochlea. The effects of discretization are much less critical when the peripheral model is used as a front-end to subsequent processing, e.g. speech recognizer or model of higher auditory centres. Discretization of the BM into 128 segments (4 per critical band) is acceptable in this case. Examples of speech cochleograms are reported in [2, 3].

The basilar membrane curves show a realistic shift of characteristic frequency/place at high levels. However, the amount of level compression at 31 dB is still short of the reported data on the real cochlea by about 10–15 dB. Increasing gain $G$ above 1 would lead to self-oscillations. Increasing $G$ to 0.999 would increase compression but result in unrealistically narrow curves at low levels. One factor limiting cochlear amplification in the current second-order cochlear partition dynamics implementation is that the real part of the BM point impedance must remain positive. Thus, there is no net gain to the travelling cochlear pressure wave as it propagates along the cochlea; the compressive effects are purely local. This problem can be alleviated if the OHC source $V_n^{ohc}(t)$ is made frequency selective, e.g. if the real part of the BM point impedance is made negative over a frequency range just below the characteristic frequency but remains positive at and above it. This points to considering cochlear partition dynamics of higher order [8].

## 6. REFERENCES

[1] A FETTWEIS, "Wave digital filters: theory and practice," *Proc. of the IEEE*, 74, pp 270–327 (1986)

[2] C GIGUÈRE & P C WOODLAND, "A composite model of the auditory periphery with feedback regulation," University of Cambridge, Technical Report CUED/F-INFENG/TR.93 (1992)

[3] C GIGUÈRE & P C WOODLAND, "Speech analysis using a nonlinear cochlear model with feedback regulation," to appear in: M COOKE, S BEET & M CRAWFORD (eds.) *Visual Representations of Speech Signals*, John Wiley & Sons Ltd., London (1992)

[4] D D GREENWOOD, "A cochlear frequency-position function for several species — 29 years later," *J. Acoust. Soc. Am*, 87, pp 2592–2605 (1990)

[5] B M JOHNSTONE, R PATUZZI & G K YATES, "Basilar membrane measurements and the travelling wave," *Hear. Res.*, 22, pp 147–153 (1986)

[6] M E LUTMAN & A M MARTIN, "Development of an electroacoustic analogue model of the middle ear and acoustic reflex," *J. Sound. Vib.*, 64, pp 133–157 (1979)

[7] T J LYNCH III, V NEDZELNITSKY & W T PEAKE, "Input impedance of the cochlea in cat," *J. Acoust. Soc. Am.*, 72, pp 108–130 (1982)

[8] S T NEELY, "Mathematical modeling of cochlear mechanics," *J. Acoust. Soc. Am.*, 78, pp 345–352 (1985)

[9] S PURIA & J B ALLEN, "A parametric study of cochlear input impedance," *J. Acoust. Soc. Am.*, 89, pp 287–309 (1991)

[10] J J ZWISLOCKI, "Analysis of the middle ear function. Part I: input impedance," *J. Acoust. Soc. Am.*, 34, pp 1514–1523 (1962)